# Analysis of Cathode Lining Failure Modes in High Current Density Cells at EGA

**Joseph Njebayi[1] and Sergey Akhmetov[2]**
1. Senior Manager Potlines
2. Senior Vice President Reduction
Emirates Global Aluminium (EGA), Al Taweelah and Jebel Ali, United Arab Emirates
Corresponding author: ndjoseph@ega.ae

**Abstract**

High-amperage cells in the Hall-Héroult process often face premature cathode-lining failure. EGA studied the life span of eight different subgroups, namely A, B, C, D, E, F, G, and H. The classification is based on electrical resistivity, flexural strength, crushing strength, and linear thermal expansion coefficient. The cathode minimum life-span across cathode grade subgroups is greater than 500 days. Grades A and B have the minimum life in high amperage cells. Statistical analysis of the premature failure rates for these groups were evaluated at 25 % and 15 % respectively while they were less than 1 % for C, D, E and 0 % for F, G, and H. Premature cathode lining failure is a major source of capital expenditure in high current density technologies. Drawing on the empirical evidence of some prematurely failed cathodes and the literature review, the purpose of this study was to establish the failure mode and effects of formation of deep potholes that shorten the life of these cells and to propose operational practices to minimize occurrences. This analysis is based on 21 theory-laden observations and measurements before and after the cathode failure. Denzin [1] and Patton [2] data sources and theory perspective triangulation were used to draw main themes. The measurements were followed by statistical correlations and interaction plot posteriori to establish the link among variables. Analysis of data indicates convergence on heterogeneous wear and formation of deep-seated potholes as the main failure mode of A and B grades. Possible factors driving heterogeneous wear include (a) thermal expansion, (b) anode spike formation, (c) fretting wear, and (d) high current density. For instance, the thermal expansion was found to be higher in A-group by a factor greater than 2 compared to F or G. Moreover, it was found that A is a high-density isotropic block whereas F is anisotropic.

**Keywords:** Cathode lining failure, cathode life, potholes, cathode wear, Denzin and Patton triangulation.

## 1. Introduction

The high erosion rate (with outliers ranging from 8 - 10 cm/year) of graphitized cathodes in high-amperage cells has become a source of financial stress for EGA. In addition to the expenses incurred in rebuilding new cathodes, the short service life and the risk of the liquid aluminium to run out of the cavity are major operational risks for smelters. In many cases, the "W- shaped" wear of graphitized cathodes appears to be the cause of failure (Nobakhtghalati [3], Reny and Wilkening [4]), but not the failure mode leading to deep-seated potholes formation. A review of cathode wear and pothole formation has been published recently [5].

This paper is a twofold-purpose study: (a) it establishes the failure modes and effects analysis (FMEA) of some graphitized cathodes in high-current density aluminium cells, and (b) it suggests the deep-pothole formation prevention to increase cell life. Given the complexity of the deep-seated pothole formation, we used a posteriori observational learning and erosion theories to guide this FMEA.

Erosion, damage, and failure mechanisms of aluminium cathode lining depend largely on the electrochemical dynamics, slurry wear, fretting, thermal dynamics and oxidative wear as failure modes. Some of these failure modes derive from the temperature gradients in the cathode blocks, thermal expansions, and fractures in the body of the blocks. At EGA, cathode blocks premature failure rate was found to vary from grade-to-grade. A and B grades premature failure rates, statistically were evaluated at 26 % and 15 % respectively while they were less than 1 % for C, D, E and 0 % for F, G, and H.

For fractures to occur on the body of the carbon block, high temperature gradients and expansion should develop followed by constraints, potentially in the opposing directions of the expansion as the block is attached rigidly to the side lining. For mechanical erosion to occur at the cathode surface, fluids and solid particles have to slide on the cathode surface continuously and with sufficient kinetic energy. For electrochemical wear to materialize, the cathode surface current density is the major cause.

Many of these cathode failure mechanisms might take place simultaneously (synergistic or chain effects) or asynchronously (isolated effects) during electrolysis. For instance, electrochemical wear may enhance slurry wear by creating deeper erosion zones and increase local current density which enhances the metal circulation. Cathode detachment may cause low resistance, increased current density, and increased electrochemical erosion afterwards.

In an effort to extend the life of the aluminium reduction cells, numerous studies have been used to improve the electrochemical resistance and characteristics of the cathode material. These studies ranged in scope from improved mechanical properties of graphitized petroleum coke cathodes to alternative shapes as well as material such as titanium diboride ($TiB_2$) for inert wettable cathodes. Yet, these efforts have neither produced significant positive results to be exploited at the industrial level, nor have they addressed the current problems of premature failure of aluminium reduction cells due to heterogeneous erosion in high-current density technologies.

In attempting to establish the cathode-lining FMEA, the one question that comes to mind is what creates deep-seated potholes (see Figure 1) at the back wall in the cathode blocks? Many researchers have endeavored to identify the possible causes of such excessive and heterogeneous abrasion. For instance, Perruchoud et al. [6] studied the coke selection criteria for abrasion resistant graphitized cathodes. They found that the excess abrasion was related to the use of low sulfur anode grade petroleum coke, which leads to a soft cathode after graphitization. They found that the selection of isotropic calcined cokes from appropriate soft pitches could allow decreasing the abrasion rate. The authors also found that dedicated coal tar pitch feedstocks used in optimized delayed coking in combination with shaft kiln calcinations have the potential to cause the “W-shaped” wear of graphitized cathodes that was found to be responsible for the cell short service life.

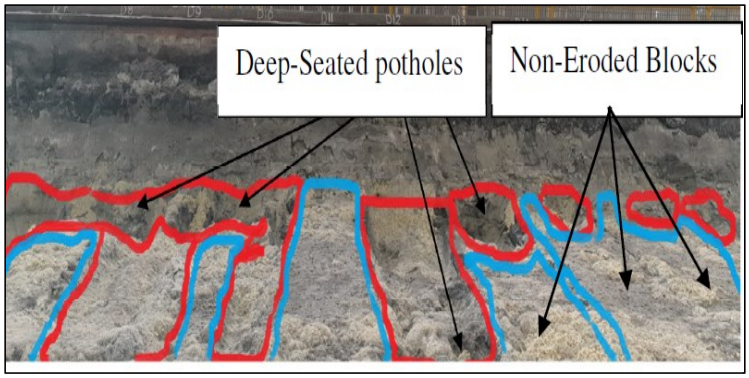


**Figure 1: Deep-seated potholes in graphitized carbon blocks.**

## 2. Methodology

In this study, we first built our knowledge through observational learning. Second, we reviewed the literature of the corrosion and abrasion theories while identifying the types of erosions and their mode of occurrence. Third, we used empirical evidence to study the cathode lining failure mode and effects analysis (FMEA) through pre-and post-failure measurements of 21-premature failed high current density cathodes. Regression analyses and interaction plot were used to identify correlation and interactions. Next, we triangulated the information and the methodology to derive main factors of premature failure. The objective was to understand the causes of deep-seated potholes formation of some graphitized cathodes in high current density cells. Finally, we discussed main factors suggested operational strategies to mitigating deep-seated potholes formation.

## 3. Literature Review

### 3.1 Empirical Evidence

The major process of cathode premature failure remains a conglomerate of complex mechanisms. Causes of cathode-lining premature failure of reduction cells are multiple and varied. Too often, they are broadly identified as no clear fundamental concepts underlie the conclusions of the investigations conducted thus far. Too often also, practitioners use potential and generic factors to draw conclusions.

### 3.2 Types of Cathode Erosion

Different types of cathode erosion exist, the most commonly known include the slurry wear, fretting and corrosion due to electrochemical reactions. Cathode decarburization may occur on the cathode surface during preheat or later on from below at the end of the blocks due to poorly sealed collector bars as shown in Figures 2 and 3.

#### 3.2.1 Cathode Decarburization

Cathode decarburization is the progressive loss of the carbon grains and formation of dust if a hot cathode is exposed to air at high temperature. Decarburization causes loss of mechanical properties of the materials resulting in dusting (Chiou and Carter [7]). The extent of the cathode decarburization will depend on the amount of air accessing the blocks, the chemical composition of the cathode, the temperature, and the quality of carbon used. The problem of air oxidation has been observed particularly in the graphitized sidewall blocks.

As for the reactions with carbon on the cathode surface during the lifetime of the pot that contribute to pothole formation, aluminium carbide formation is the main electrochemical reaction [5]. Another mechanism suggested by Øye [8] is that un-dissolved aluminium fluoride deposited at the cathode may react with the carbon to form aluminium carbide.

Based on these erosion modes, resistance to the cathode decarburization mechanism should be centered on five type actions:

- Controlling operating temperature of electrolyte cell and operation within design specifications,
- Increasing alumina dissolution to prevent accumulation of sludge and solid ridge on the cathode surface,
- Sealing well collector bar windows to limit air ingress and prevent oxidation of carbon blocks near sidewalls,
- Proper precautions during start-up, shutdown, and cell restart.

Cathode surface coating may prevent the chemical reactions at the surface to take place.

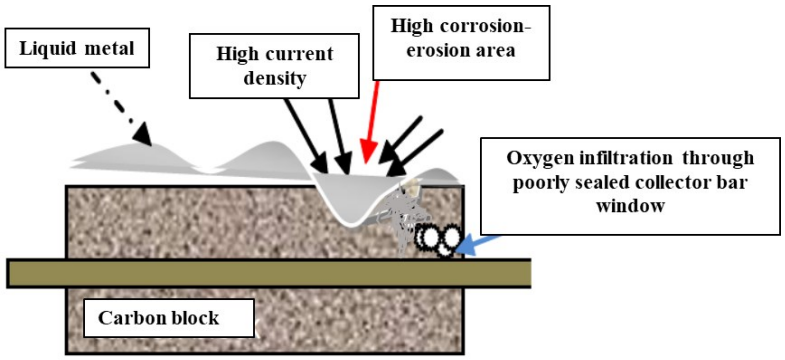


**Figure 2. Illustration of pothole formation from the cathode surface and decarburization damage due to air infiltration through the collector bar windows.**


**Figure 3. Potential area of air penetration through collector bar window.**

### 3.2.2 Temperature Gradients Causing Cracks and Deep Potholes

High operating temperature such as during an anode spike can lead to local decarburization through excessive heat generation. The situation can be worse in the case the total height of the spike (see Figure 4) meets the cathode surface. The local current density of the active area can reach more than 200 – 300 % of the nominal levels . This active area would be short-circuited, leading to hot spot, high temperature gradients, thermal stress, and cathode fractures. The larger the temperature difference the higher the stress in the cathode block. Theory shows that the total

stress in the material in the context of temperature change is calculated by $\sigma = E\lambda(T_o - T_b)$ Where E is the Young's modulus of the carbon bloc, λ is the thermal expansion coefficient and $T_0 - T_b$ is the temperature difference over a certain distance from the spike center to the bulk carbon block. A severe anode spike in contact with the cathode block can increase the temperature gradient at the cathode surface by 5 – 15 %, equivalent to $T_0 - T_b$=50 °C to 150 °C.

Given that the space to accommodate the thermal expansion of the carbon block is limited due to the sidelining configuration and prior sodium diffusion-expansion, it can be anticipated that the carbon block would be susceptible to cracking at the active area of constraints.

Figure 5 shows a carbon surface with deep-seated potholes (outlined in yellow) about 25 - 30 cm deep near the end of the carbon blocks under the shadow of a spike. It was established statistically that 90 % of the anode spikes occurred at the backside (towards the end of the blocks) and that is where the deep-seated potholes were located. In summary, there is coincidence (correlation) not causation between the deep potholes and anode spikes. Ideally, the anode spike should not reach the cathode level; its formation should be discovered earlier and the current through the spike disperses in the metal pad before it reaches the cathode block.

Areas of cracks and erosion lead to lower the local electrical resistance of a block, which increase the current density, polarization, electrochemical reactions and erosion. Cathode cracks can also change the local dynamics of the metal flow, which creates local vortices and aggravates the erosion rate.

**Figure 4. Extended anode spike.**

**Figure 5. Deep-seated potholes in a graphitized cathode.**

### 3.2.3 Operating Conditions and Current Density

The quest for high productivity has forced aluminium smelters to increase potline current, sometimes beyond the nominal limits of the technological capability. Notwithstanding, increasing the current at constant cathode cross sectional area has detrimental effects on electrochemical erosion due to the increased current density on top of cathode carbon, material expansion and the dynamic frictions between the fluids and the cathode surface.

The increased current density also affects thermal equilibrium of the pots, which may directly affect pot life and cause premature cathode failure through the side wall, not related to cathode

erosion or pothole formation. Figure 6 shows the regression of the sidewall temperature as a predictor of internal heat or current density shift during different phases of the amperage increase. The average sidewall temperature rose to 430 °C (standard deviation (SD) = 15 °C) when the current density increased to 1 A/cm$^2$. Below 0.9 A/cm$^2$, the average sidewall temperature ranged from 370 - 375 °C (SD= 10 °C), about 50 °C upward shift for additional 0.1 A/cm$^2$. Premature lining failure was noticed a few months later after the electrical current density was 1 A/cm$^2$ and above. Figure 6 also shows the correlation between the current density (heat flux) and sidewall temperatures.

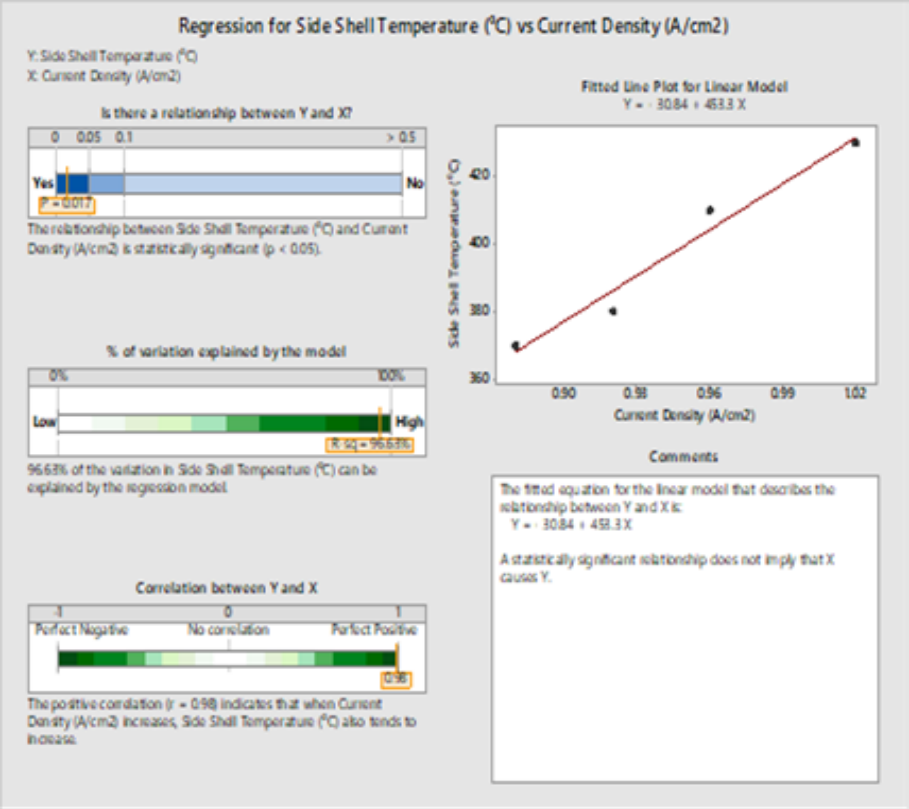

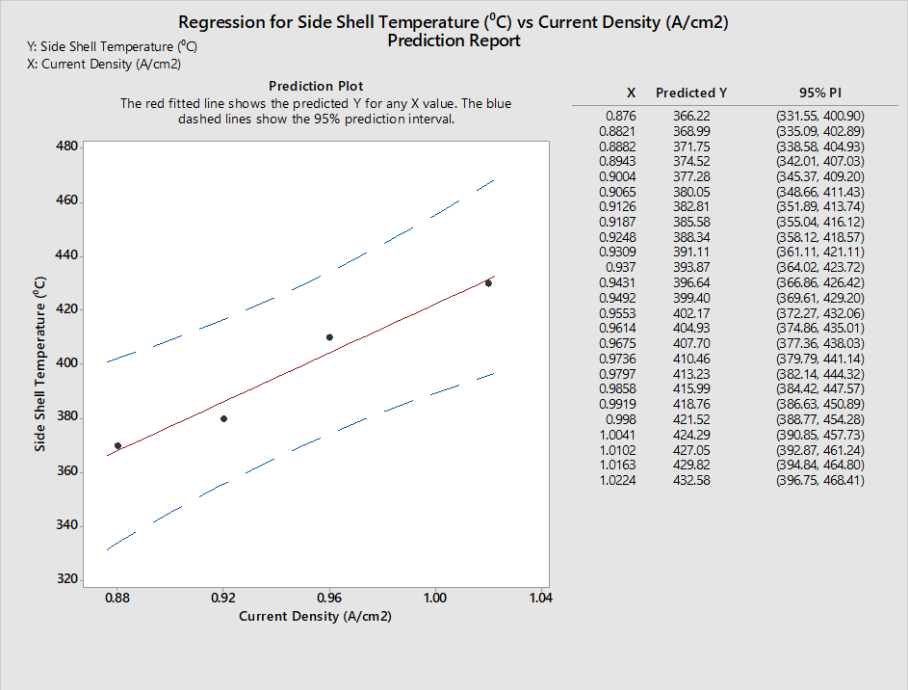


| X | Predicted Y | 95% PI |
|---|---|---|
| 0.876 | 366.22 | (331.55, 400.90) |
| 0.8821 | 368.99 | (335.09, 402.89) |
| 0.8882 | 371.75 | (338.58, 404.93) |
| 0.8943 | 374.52 | (342.01, 407.03) |
| 0.9004 | 377.28 | (345.37, 409.20) |
| 0.9065 | 380.05 | (348.66, 411.43) |
| 0.9126 | 382.81 | (351.89, 413.74) |
| 0.9187 | 385.58 | (355.04, 416.12) |
| 0.9248 | 388.34 | (358.12, 418.57) |
| 0.9309 | 391.11 | (361.11, 421.11) |
| 0.937 | 393.87 | (364.02, 423.72) |
| 0.9431 | 396.64 | (366.86, 426.42) |
| 0.9492 | 399.40 | (369.61, 429.20) |
| 0.9553 | 402.17 | (372.27, 432.06) |
| 0.9614 | 404.93 | (374.86, 435.01) |
| 0.9675 | 407.70 | (377.36, 438.03) |
| 0.9736 | 410.46 | (379.79, 441.14) |
| 0.9797 | 413.23 | (382.14, 444.32) |
| 0.9858 | 415.99 | (384.42, 447.57) |
| 0.9919 | 418.76 | (386.63, 450.89) |
| 0.998 | 421.52 | (388.77, 454.28) |
| 1.0041 | 424.29 | (390.85, 457.73) |
| 1.0102 | 427.05 | (392.87, 461.24) |
| 1.0163 | 429.82 | (394.84, 464.80) |
| 1.0224 | 432.58 | (396.75, 468.41) |

**Figure 6. Regression of the sidewall temperature vs. current density.**

### 3.2.4 Slurry Wear

Slurry wear is a progressive loss of material from the cathode surface by the friction with solid materials. For a reduction cell, the liquid carriers are aluminium and electrolyte; bath and the solids carried are usually hardened-anode cover material, crust and coagulated alumina mixed with bath.

Figure 7 shows the shape of the flow in potholes. Observations of the shape of the potholes indicate that the fluid might have been turning around forming a vortex, which is driven by increased current flow into the pothole. These vortices increase erosion through slurry wear and through rapid removal of aluminium carbide that forms there. The location in the cell is an important factor of the vortex creation and slurry erosion; it has been observed that they are more frequently found opposite to anode risers (i.e., downstream).

**Figure 7. Erosion pattern and indication of vortices.**

Kelvin-Helmholz theory shows that the flow velocity is higher close to its recirculation axis and decreases in inverse proportion to the distance from the axis. The velocity difference between the circulating fluid and the fixed cathode induces the drag which is responsible for cathode wear in the pothole. The magnitude of the drag between the liquid metal and the cathode surface depends on the shape or geometry of the pothole.

### 3.2.5 Fretting

#### 3.2.5.1 Definitions

Fretting is a mechanical wear of a cathode that occurs during oscillatory movements between the cavity-cleaning shovel and the cathode surface. These types of oscillatory movements and fretting are generally tangential to the cathode and occur during anode setting. Fretting can be a catalyst for slurry wear as it accelerates material damage at the interface of two contacting surfaces. One effect of fretting wear is its contribution to material fatigue (Geitner and Bloch [9]). The surface damage caused by fretting wear might facilitate crack formation and furthermore, deep-seated potholes. Geitner and Bloch found that factors that influence fretting wear include the frequency and duration of fretting, the load, or pressure applied, and the hardness of materials.

Examinations of surface fractures of premature failed cathodes (see Figure 9) have shown that cracks originate from both electrochemical wear and mechanical contacts near the edge of fretted cathodes. The worn cathode surfaces and debris were also examined to understand the mechanism of failure. No one-failure mode could explain the entire quantitative and qualitative wear characteristics. Most locations at the cathode edges showed similar frictional behavior and fractures. Importantly, as the cathodes erode in heterogeneous manner, the shovel edges interlock with the valleys of the rough cathode surface during pot-cavity cleaning, which produces more force to push leading to breakages.

#### 3.2.5.2. Fretting Tests

We measured the shovel stroke at the cathode-lining workshop in order to understand the possible influence of the shovel oscillatory frictions on the cathode deep-seated potholes. The stroke is the total vertical travelling when an operator decides to lower the shovel from top to the bottom of the anode cavity. The pot tending machine shovel (see Figure 8) has sharp edges and the two metallic buckets composing the shovel operate in a circular dynamic movement (CDM). The sharp edges, in addition to the CDM compared to a linear displacement of the buckets can create impingement of the fretted material. The magnitude of impingement depends on the load at the cathode surface and the hydraulic pressure exerted. The changing altitude and horizontal displacement of the shovel edges cause the CDM. A linear displacement potentially would allow smooth frictional results.

**Figure 8. Pot tending machine scoop.**

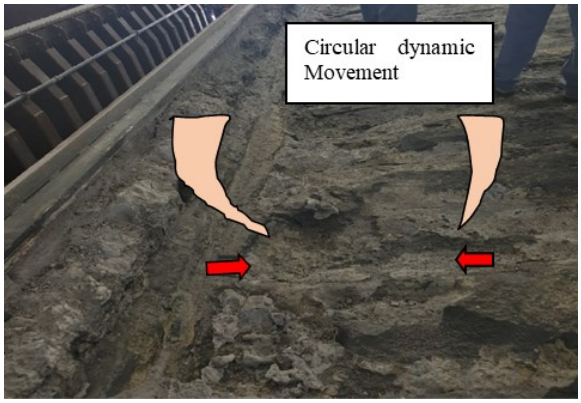


**Figure 9. Example of fretting wear.**

The shovel stroke can be parameterized depending on the operational requirements as well as the cathode height (see Table 1). While the maintenance teams often maintain a clearance of 5 mm between the fretted surface and the shovel sharp edges, there are instances where cathode height increases over time upon operational requirements and specific design. Increased cathode height should initiate the shovel stroke re-parameterization. Discrepancy often occurs when plant-change management process is not applied. An observation of Figure 9 shows that the cathode-surface wear was most severe in the locations of cavity scooping. Most samples analyzed showed pitting, electrochemical erosion and delamination. Wear rates and delamination were significantly higher in impingement locations.

**Table 1. Fretting and impingement test.**

| **Test 1** | **Total stroke (mm)** | **Initial operational stroke (mm)** | **Initial clearance (mm)** | **Initial cathode level (mm)** |
|---|---|---|---|---|
| | 4855 | 4850 | 5 | 0 |
| **Test 2** | Total stroke (mm) | New operational stroke (mm) | New clearance (mm) | New cathode level upward (mm) |
| | 4855 | 4850 | **-8** | **+13** |
| **Comments** | | The operational stroke should decrease to 4837 mm. | The scoop exerts a hydraulic (fretting) force or pressure equivalent to 8 mm downward and tangentially to the fretted material. | |

### 3.2.6 Electrochemical Erosion

Electrochemical erosion is an exchange of electronic charges. These reactions soften the surface of the cathode and may yield aluminium carbide. The formation and dissolution of aluminium carbide is an important factor of cathode wear. Nobakhtghalati [3] found that the formation of carbides is influenced by the current density.

Aluminium carbide is commonly found in autopsied pots and its role in cathode wear is widely recognised in the literature [5]. It is formed according to Equation (1), possibly with some intermediate reactions and is removed by dissolution in bath, which allows the reaction to take place continuously.

$$4Al(l) + 3C \rightarrow Al_4C_3 \quad (1)$$

### 3.3 Deep-Seated Pothole Formation Mechanisms Summary

Conceptually, the deep-pothole formation in the cathode block can be summarized in the diagram outlined in Figure 10. The process steps are numbered from (1) to (10). The selected numbering order is, according to our view the most probable scientific explanations to describe the deep-seated pothole formation. Extended anode spike, even though it is rare, is pointed out as possible cause of deep-seated pothole formation through the mechanism of local overheating, thermal stress on the cathode, boundary busting, reduced block height, and increased current density and erosion.

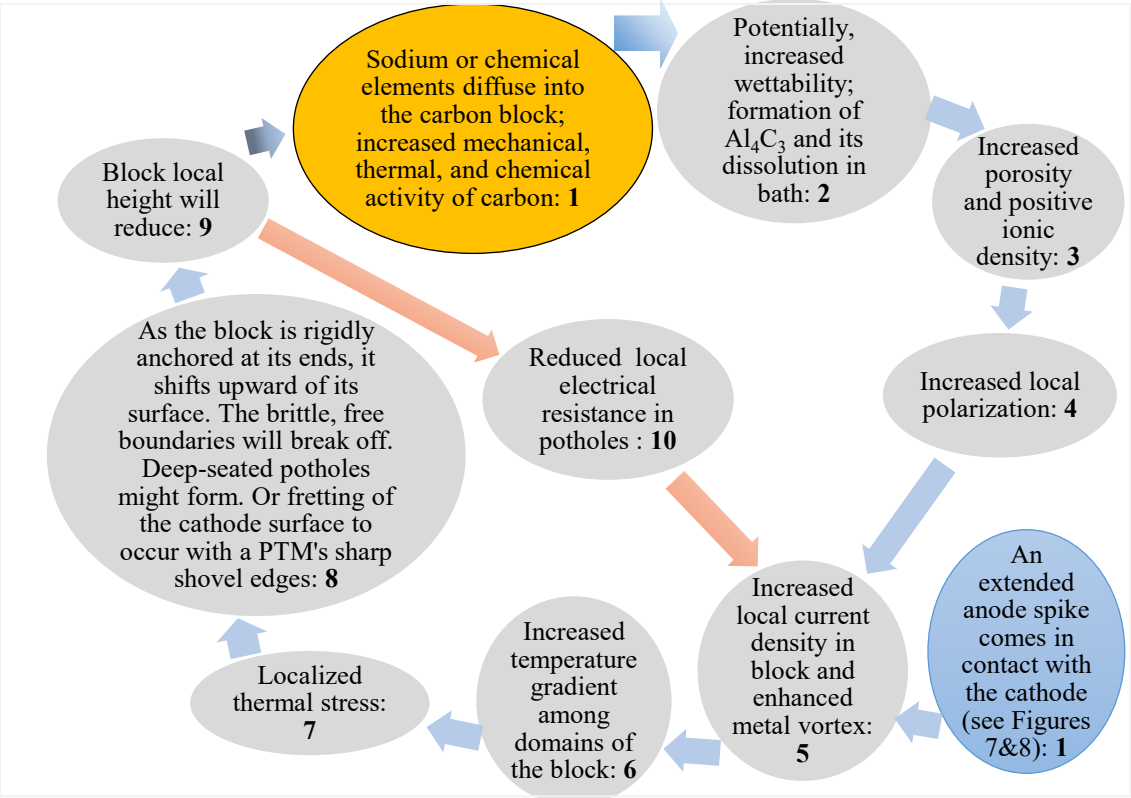


**Figure 10. Deep-seated potholes formation: Physical and electrochemical mechanisms.**

## 4. Measurements, T-Test, ANOVA, Triangulation and Results

### a. Electrical Resistivity Discrepancy among Carbon Blocks

A statistical test (paired t-test) was conducted to evaluate the mean difference between paired measurements of the cathode erosion depth on upstream and downstream of a high-density reduction cell technology. We assumed no-erosion depth difference between the two groups within 95 % confidence interval. ($H_0$: $\mu_d = \mu_u$) where $\mu_d$ and $\mu_u$ were the means of the two groups of measurements. The data were collected from 15-premature failed cathodes of age 1100 - 1400 days. The measurements were done at 30 locations targeting the areas with high frequency of liquid aluminium leakage, near misses and minimal erosion. Each block in consideration was

measured in two locations, one upstream and one downstream. The results are summarized in Table 2.

**Table 2. Paired T for upstream erosion depth - downstream erosion depth (cm).**

| | N | Standard deviation | SE | Mean |
|---|---|---|---|---|
| Upstream erosion depth | 15 | 18.66 | 9.38 | 2.42 |
| Downstream erosion depth | 15 | 23.85 | 10.09 | 2.60 |
| Difference | 15 | -5.19 | 8.89 | 2.30 |

T-Test of mean difference = 0 (vs ≠ 0): T-Value = -2.26 P-Value = 0.040; 95 % CI for mean difference: (-10.12, -0.27).

The test indicated that the means of the total erosion depth in up and downstream were statistically different (see Figure 11, $\mu_d - \mu_u = 5$, P-Value = 0.040). The standard deviation was 10 in the downstream and 9 in the upstream. The high standard deviation was revelatory of heterogeneous erosion among blocks. The outlier observed for the erosion rate was around 9.5 cm/year.

Figure 11 shows the histogram of the erosion difference within blocks. The maximum difference measured was 10 cm with outliers ranging from 15 – 20 cm. The histogram also shows that the erosion difference (upstream – downstream) was asymmetric with a few values only on the right side (positive skewness). The confidence interval for the mean outlined in the boxplot (Figure 12) confirms this finding. These data revealed that a systemic factor drives the erosion downstream.

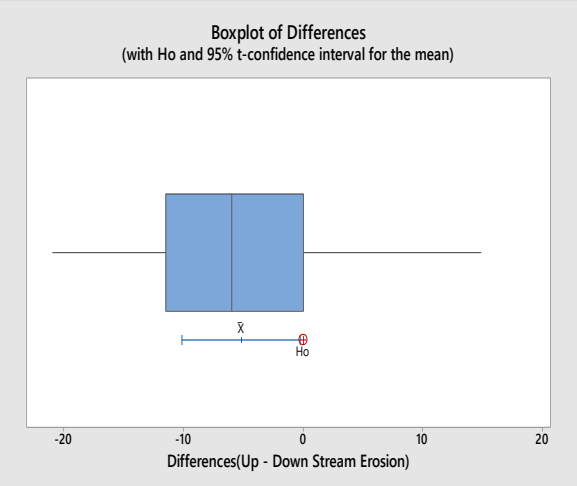


**Figure 11. CI for the erosions (Upstream – Downstream).**

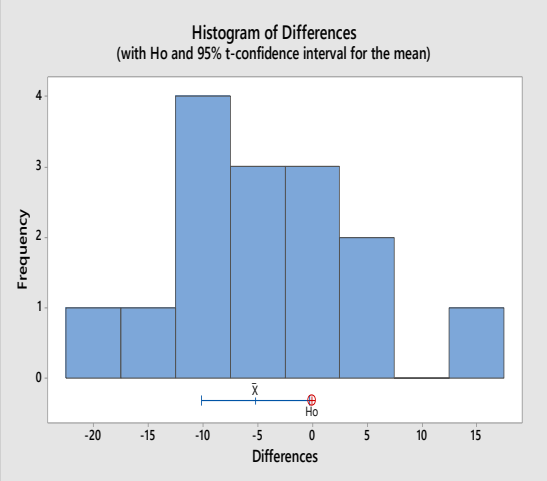


**Figure 12. Erosion difference within block (Upstream - Downstream).**

**b. Triangulating Statistical Findings with Other Observations**

Figure 13 shows that over 55 – 60 % of the carbon blocks had less erosion than other areas and we may assume that these areas probably carried less current than the areas of deeper erosion. As

indicated through the black arrows, the current probably shifted from one block to another or from a portion of a block to another one.

Through a posteriori knowledge, three inferences may be used to interpret such cathode behavior: (a) the blocks casting quality was poor, leading to resistance variations across blocks; (b) poor operating practices led to excessive sludge build up and derived horizontal current. (c) Third, the problem can be due to carbon block inhomogeneity and variation of the block resisitivity. (d) Finally, we consider also synergistic effects of (a), (b), and (c). Research shows that graphite resistivity is based on the directional orientation of the carbon structure.

Figure 14 shows a thermal image (TI) of a prematurely failed cathode. The TI outlines areas with high electrochemical activity, cracks, aluminium carbide traces (yellowish colour) and areas with low electrochemical activity potential (bluish). Assuming that all objects emit infrared energy (heat) as a function of their temperature, the thermal sensor allowed collecting the infrared radiations from different areas of the cathode surface to create a comprehensive electronic image that differentiates erosion patterns. The electronic image corroborated other observations and measurements of the erosion pattern. Results indicated that the slightly blue tinge was the dominant colour, covering 45 – 50 % of the area; it was assumed that these were areas with less conductivity. The yellow tinge covered about 30 – 35 % whereas the reddish colour covered less than 10 – 20 %. The electronic image shows that the cathode surface is the seat of different conductivities and reactions.

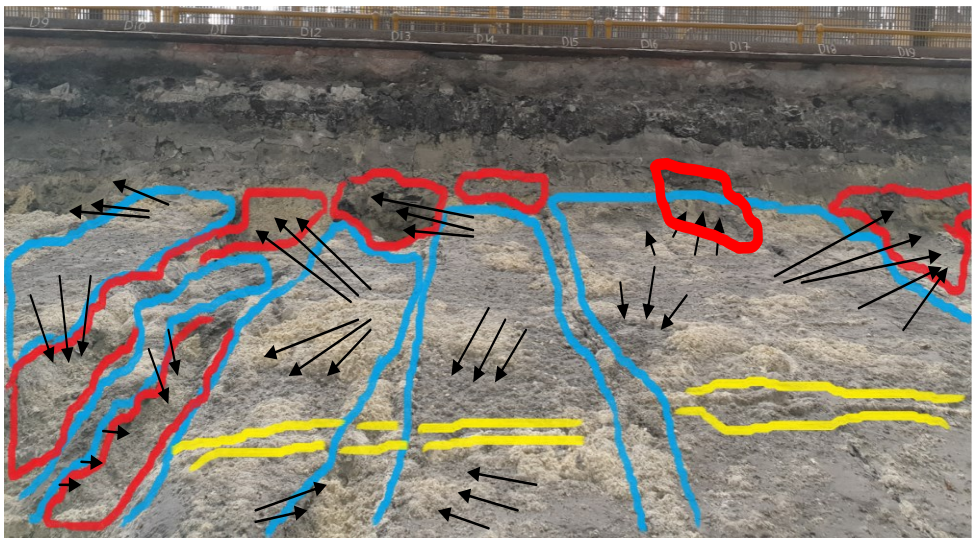

**Figure 13. Deep-seated pothole formation is enhanced by possible current flow into high erosion areas.**

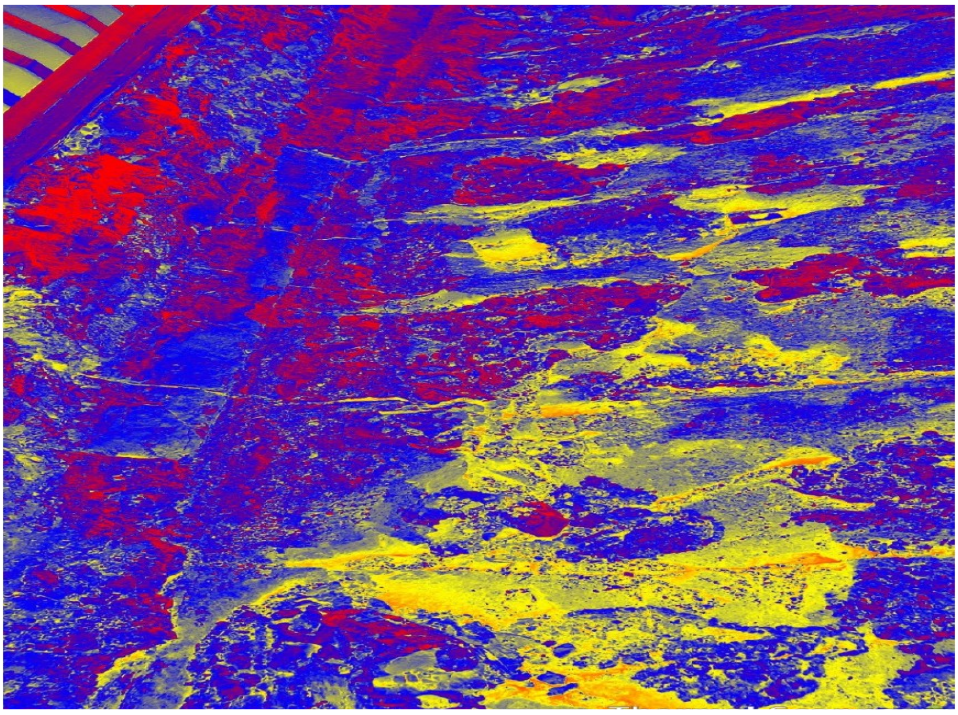

**Figure 14. Thermal imaging of a prematurely failed cathode.**

On the other hand, casting quality can affect the electrical conductivity of the assembled carbon block and steel bar. Conditions such as the quality and composition of the cast iron, the cooling rate, and the mechanical handling of the assembly can also affect the integrity of the bonding. Mechanical handling can generate micro cracks, which produce high resistivity.

## 5. Comparison of Two Prematurely Failed Cells

Figures 13 and 15 are two similar patterns drawn from two different prematurely failed cells. Figure 13 shows that the erosion within block in this cell was more homogeneous compared to Figure 15. In the former, 30 – 40 % of the blocks had minimal erosion less than 15 % whereas in the latter, 50 – 60 % exhibited a similar rate.

Typically, these two lining arrangements exhibited similar deep-seated potholes formation at the ends of the carbon blocks. A close investigation of the type of failures shows both, the mechanical failure (sharp cutting edges, breaking apart patterns) and electrochemical erosion (dissolved, discoloration, and changing of the crystal structure). In addition, the blocks showed highly heterogeneous erosion within blocks and from block to block. This heterogeneity shows the absence of linearity of the resistivity; which reflects the failure modes (a), (b), and (c) discussed previously.

Figure 16 shows that some of the carbon blocks and collector bars might not have carry much current because there has been little sodium diffusion to the outside. This observation was correlated with the carbon cathode erosion pattern. Results indicated that the rate of erosion of such carbon blocks was smaller than the rest. Part of the non-conductivity can be explained through the three failure modes outlined above.

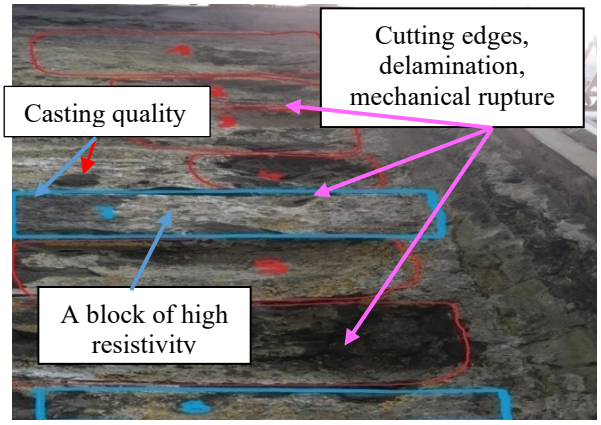


**Figure 15. Cathode deep-pothole formation.**

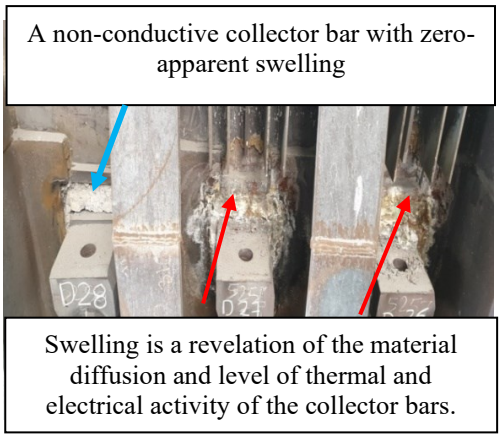


**Figure 16. A nonconductive-vs. conductive collector bars**

## 6. Potlining Premature Failure Statistics

Table 3 shows the statistics of the cell lining failures of 24 cells. The data show that most of the failures were located on the downstream of the cell. Most premature failures were due to deep-seated potholes. Of the total cathode failures, 29 % failed from the upstream, 12.5 % had end burst and 58.3 % occurred from the downstream (see Figures 17 and 18). The relative risk factor of failure was twice higher in downstream than upstream. End bursts are a consequence of adverse factors such as high internal heat, end wall lining failure, and operating conditions (e.g., material accumulation).

Similarly, 58.3 % of the failures occurred from the end blocks and 41.7 % from the middle blocks. End blocks are the last six of each end. The end blocks compose 42.8 % of the total number of blocks but contribute for 58.3 % of the cell lining premature failures (see Figure 19). The relative risk factor to failing from end blocks is 39 % (58.3/41.7) higher than the middle ones. The risk factor is any inherent attribute, characteristic, or exposure that increases the likelihood of developing abnormal erosion leading to cathode failure. Figure 18 shows actual failures as well as the near misses cases registered. Near misses are cases that had strong potentiality to fail, but which operation teams identified and neutralized before occurrence. The data showed similar findings.

**Table 3. Lining failure statistics.**

| | **Frequency of failure in %** | **Frequency of failure including near misses in %** |
|---|---|---|
| Upstream | 29.17 | 33.33 |
| Downstream | 58.33 | 54.90 |
| End burst | 12.50 | 11.76 |
| | | |
| End blocks | 58.33 | 59 |
| Middle blocks | 41.67 | 41 |
| Sample size (n) | 24 | 51 |

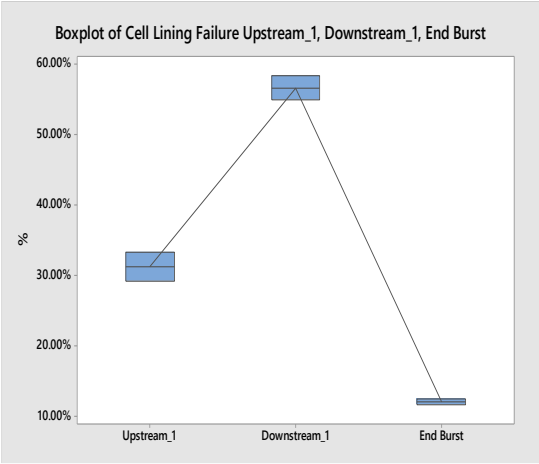


**Figure 17. Lining failure distribution.**

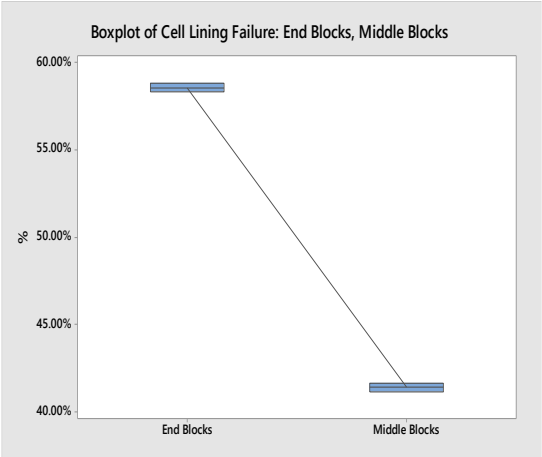


**Figure 18. Lining failure distribution: Middle vs end blocks.**

The total sample size including the near misses was 51. 53 % of these were near misses. Downstream showed higher occurrence potential than upstream. Based on the similarity between the actual failure and the potential failure frequencies, one may conclude that this behavior was partly inherent to the design (magnetic, electric and magnetohydrodynamics of the cell). Nevertheless, the spread of the occurrences across the blocks implies a common cause within the material grade, resistivity of the blocks, or operational practices. Because this failure concerns only some of the cathode grades namely A and B, one may conclude that the geographic location was a contributing factor. A special cause exists thereafter within these grades.

The particularity of these grades is that they have smaller resistivity, high thermal linear expansion and some are isotropic. For instance, the thermal linear expansion ratio of A to C was calculated at 1.8; notwithstanding, the sidelining configuration does not differentiate or consider such discrepancy. Typically, nine different grades are installed; only two are prone to high premature failure rate (see Figure 20).

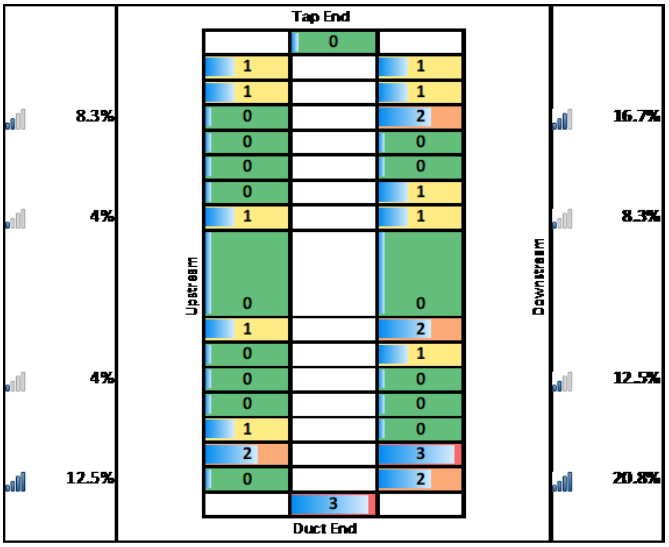


**Figure 19. Location frequency of actual cathode failures (%) and cathode failure potential.**

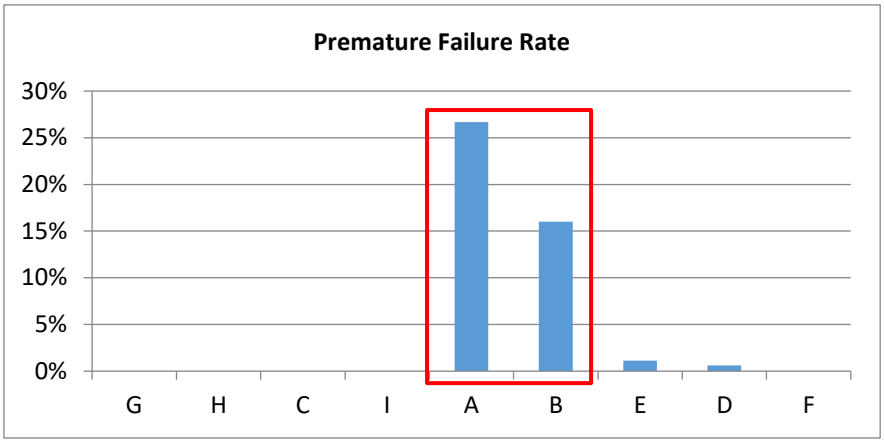


**Figure 20. Cathode grade-based premature failure rate.**

## 7. Discussion and Proposed Solutions

Data and method triangulation of empirical evidence allowed isolating main factors of deep-seated pothole leading to premature failure. We found multiple factors, potentially driving the cathode pothole formation. Some factors had more weight. The cathode grade, thermal linear expansion, flexural strength, current density, and the sidelining configuration are among the most important contributors. Fretting and slurry wear, casting quality, geographic location, and anode spikes were the second most important factors of deep-seated potholes formation.

Figure 21 summarizes the effect and the potential interactions among factors. Although not all factors are analyzed, most of them are displayed in the matrix. To better visualize Figure 21 and its legend, please zoom it to 200 %. The data have been normalized to perform the interaction plot in order to reflect the percentage of actual values within the specification scale of each cathode grade. Factors such as technology, current density, the local Reynolds number, fretting, and slurry were assumed to induce common effects on all cathode grades. Factors with attribute features had two levels: “Yes”, when an observation yielded an effect, “No”, when no effects were noticed. For instance, where no premature lining failure was observed, the deep-seated pothole factor was set to “No”; on the contrary, it was “Yes”.

From the material perspective, high flexural strength, low thermal expansion coefficient, and anisotropy properties should be desired to mitigate deep-seated pothole formation. Should a company make a decision to use materials with high thermal linear expansion, the sidewall lining needs to be adjusted to have free space available for block expansion.

Low electrical resistivity and high thermal linear expansion seemed to interact. Potentially, in high current density conditions, vertical current density into increases towards the side walls, leading to portions of the blocks overheating, expanding and delaminating, which subsequently was worsened through fretting and slurry wear. High flexural strength might be needed to withstand block delamination. High-density block seems to correlate with low electrical resistivity (see upper-third column), which can be explained physically through the atomic arrangement and crystal structure.

Materials having isotropic features (e.g., A grade, fourth column) may need proper structural arrangement during the lining because they have multiple axial stress failures. For instance, research shows that the heat flux vector is not perpendicular to the isothermal surface in anisotropic material (Su et al. [10]), which is a significant advantage compared to isotropic

material. In addition, they. found that the magnitude of heat transfer rate of anisotropic material in one direction is relevant to both the temperature gradient in this direction and the temperature gradient perpendicular to it.

Finally, anode spike was found to be a common factor, particularly it interacted with low resistivity cathode grades. The high anode-spike occurrence in these cathode grades can be linked to the resistance set point balancing .

We found that premature lining failure was high in cathode grades A and B, 26 and 15 % respectively. Statistical analysis indicated high correlation between current density and sidewall temperature. High current density increases electrochemical erosion, carbide formation, and thermal expansion. Side lining configuration should be adapted in accordance to each cathode grade thermal expansion coefficient. Companies operating high-current density reduction cells should avoid these cathode grade types.

High current density also increases horizontal currents, which change the metal flow dynamics. The flow depends on the location in the cell. Observations of some potholes indicated that the liquid metal was turning around in a vortex, which increased erosion. The greater the speed, the higher the erosion. However, liquid recirculation cannot create cathode fracture with sharp edges.

Finally, cathode block casting quality is a factor in electrical resistance discrepancy and the erosion pattern within a block and among blocks. Although this factor was not captured in the interaction plot matrix, some pictures of heterogeneous erosion within the same collector bar revealed poor contact between carbon and collector bars. The measurement of the resistance should be conducted upon receiving the blocks from the supplier and after casting (see Figure 23). These measurements allow verifying the compliance of the material to contractual specifications as well as compliance to the standard procedure. Any deviations beyond the contractual agreements or critical limits should not be used or should be used with circumspection based on appropriate cell lining procedure.

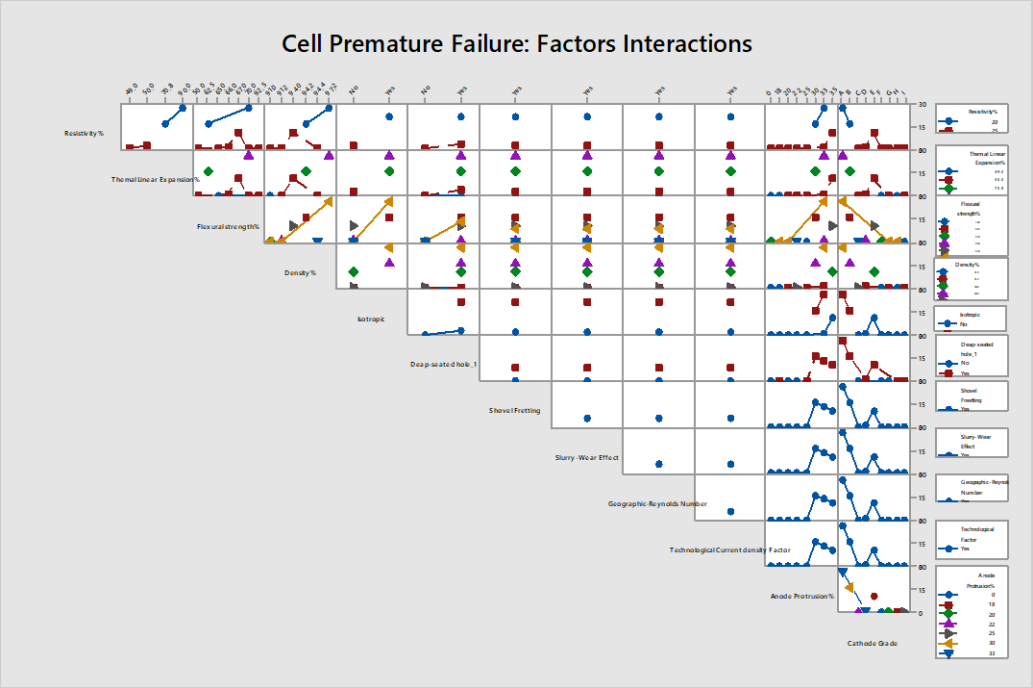


**Figure 21. Analysis of premature failure: Interaction plot.**

After collector bar casting, the measurements of the total resistance should be conducted (Figure 22). The technical team should establish acceptable limits beyond which disassembling and recasting should be considered. Next, the assembled blocks should be grouped by resistivity similarity (repeatability) at 95 % confidence interval. Blocks for which the total resistivity difference exceeds 5 – 10 % should not be associated (see Figure 23). Next, as we found that most deep-seated pothole formation and premature failures occur at the ends or close to end blocks, install blocks with higher resistivity where high erosion rate was observed.

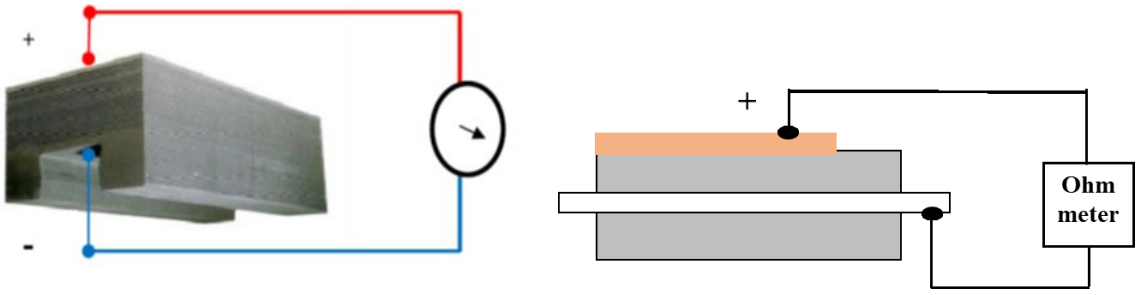


**Figure 22. Measurements of the cathode block resistivity (left) and of the resistance of the assembly carbon block-collector bar (right).**

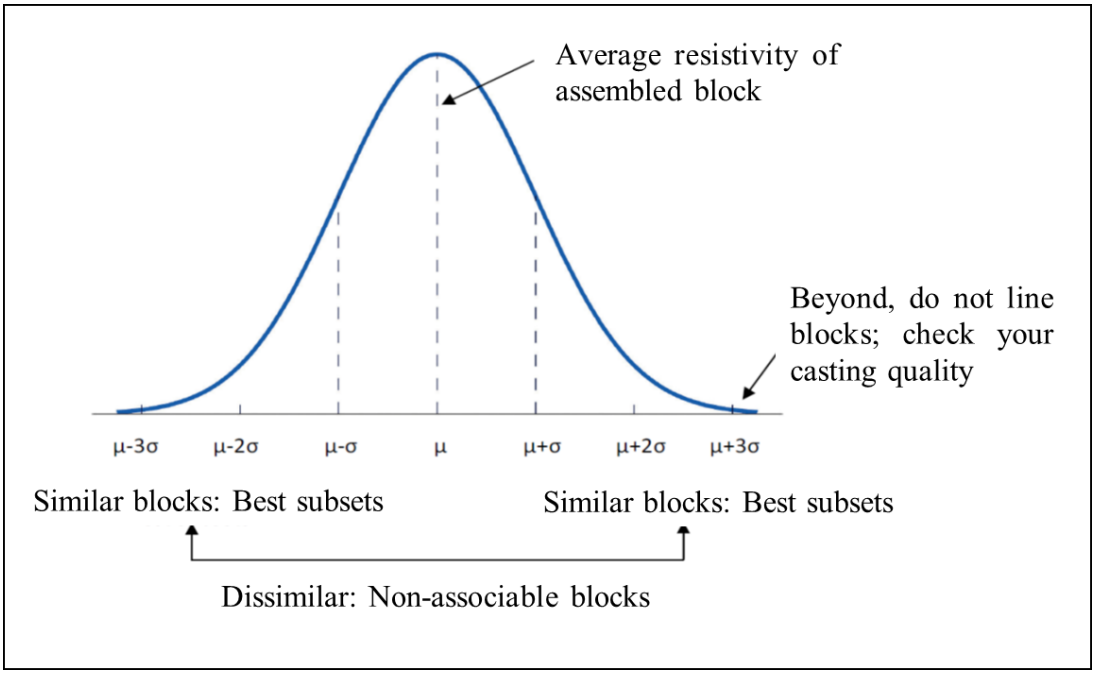


**Figure 23. Measurements of cast block resistivity and lining strategy.**

## 8. References

1. Norman K. Denzin, Triangulation 2.0, *Journal of Mixed Methods Research*, 2012 *6*(2), 80-88. https://journals.sagepub.com/doi/abs/10.1177/1558689812437186?journalCode=mmra

2. M. Q. Patton, Enhancing the quality and credibility of qualitative analysis, *HSR: Health Services Research* 1999 34 (5) Part II, 1189-1208.
3. Saeid Nobakhtghalati, Wear of carbon cathode lining in aluminium electrolysis cell: The effect of rotation speed in laboratory test cell, *Master's Thesis, NTNU*, Institutt for materialteknologi, 2014.
4. Pierre Reny and Siegfried Wilkening, Graphite Wear Cathode Study at Alouette, *Light Metals* 2000, 399-404.
5. Samuel Senanu, Tor Grande, Arne Petter Ratvik, Role of pitting in the formation of potholes in carbon cathodes – A review, Proceedings of 34th International ICSOBA Conference, Qubec City, Canada, 3 – 6 October 2016, Traavaux 45, Paper AL31, 787-796.
6. Raymond Perruchoud et al., (2011). Coke selection criteria for abrasion resistant graphitized cathodes, *Light Metals* 2011, 1067-1072.
7. W.C. Chiou Jr, and E.A. Carter, (2003). Structure and stability of $Fe_3C$-cementite surfaces from first principles. *Surface Science, 530(1-2),* 2003, 88-100. Available at https://doi.org/10.1016/S0039-6028(03)00352-2
8. HaraldA. Øye, Materials used in aluminium smelting, *Light Metals 2000*, 3–15.
9. Fred K. Geitner, Heinz P. Bloch*, Machinery Failure Analysis and Troubleshooting (Fourth Edition), 2012*
10. S. Su, J. Chen, and C. Zhang, Study on Performance of Anisotropic Materials of Thermal Conductivity. *The Open Civil Engineering Journal, 2011, 5, 168-172.* Available at https://pdfs.semanticscholar.org/4757/84d7f1a2eabd7a0e1185d1eedc8a7dd4bbf1.pdf